

# Atomic Disorder, Magnetic property and Thermal vacancy formation Co based Heusler Alloys $\text{Co}_2\text{MnZ}$ ( $\text{Z}=\text{Si}, \text{Ge}, \text{Sn}$ )

Inamul Haq Wani<sup>1</sup>, Aayushi Sharma<sup>2</sup>, Indu Sharma<sup>3</sup>, Mohd Shafiq<sup>4</sup>, Brij Bir Singh<sup>5</sup>, Sushila<sup>6</sup>

Department of Physics, Vivekananda Global University Jaipur, Rajasthan, India<sup>1,6</sup>

Department of Physics Maulana Azad Memorial College, Jammu, Jammu and Kashmir, India<sup>2,3,4,5</sup>

Corresponding Author: [Inamwani123@gmail.com](mailto:Inamwani123@gmail.com)

**Keywords:** Full Heusler Alloys, Magnetic Properties, Atomic Disorder, Thermal Vacancy

## ABSTRACT:-

Co type and MnZ type at atomic and magnetic disorder are investigated for Co based Heusler alloy  $\text{Co}_2\text{MnZ}$  ( $\text{Z}=\text{Si}, \text{Ge}, \text{Sn}$ ) as a function of quenching temperature. It is shown that Co type disorder preferentially proceeds with increase in quenching temperature while the MnGe type disorder preferentially proceeds in  $\text{Co}_2\text{MnGe}$ . In  $\text{Co}_2\text{MnSn}$  only the Mn-Sn type disorder proceeds. On the other hand decrease with in quenching temperature  $\text{Co}_2\text{MnGe}$ , while it remains almost constant  $\text{Co}_2\text{MnSn}$ .

## 1. INTRODUCTION:-

Co-based heusler type ferromagnetic alloys with the chemical formula  $\text{X}_2\text{YZ}$  (where  $\text{X}=\text{Co}$ ),  $\text{Y}=(\text{Cr and Mn})$  and ( $\text{Z}=\text{Si}, \text{Ge}, \text{Sn and Al}$ ) such as  $\text{Co}_2\text{CrSi}$ ,  $\text{Co}_2\text{MnGe}$  and  $\text{Co}_2\text{CrAl}$  are prospective candidate for application in the spin electronic devices because these are theoretical prediction to be half metal ferromagnets with 100% spin polarization due to a gap at the Fermi level is the minority spin band. Despite the theoretical prediction it is difficult demonstrate the half metalicity for these compounds. Some factors such as atomic disorder, nonstoichiometry and oxidation in the bulk and oxidation in the bulk and interface are thought to leave degradation of the half metalicity. The heusler ( $\text{L}_{21}$ ) ( $\text{Co}_2\text{YZ}$ ) type structure with having four FCC

sublattices shown in fig1. It can also be regarded as the structure consisting of 8 BCC position in unit cells occupied the corner position. Co-sites are occupied by Co atoms by 8 bcc position are occupied alternatively Y atoms (Y site) and Z atoms (Z sites). Atomic disorder occurs by deviating the composition from the stoichiometry or by elevating temperature from 0k. Effect of the atomic disorder on the magnetic property as well as half metallicity in half heusler alloys  $\text{Co}_2\text{YZ}$

As we studied half heusler alloy and full heusler alloy leads to the former type of disorder is predicted to lead the degradation of magnetism as well as half metallicity as the latter type does not significantly affect the properties. A degree of atomic disorder can be well controlled by quenching from appropriate temperature because it varies depending on temperature  $T$ . We have studied experiment magnetic behavior and atomic disorder in B2-type  $\text{Co}_{1-x}\text{Fex}$  alloys ( $0.4 < x < 0.6$ ) and B<sub>2</sub> and heusler type  $\text{CoFe}_{1-x}\text{Al}_x$  alloys ( $0 < x < 1$ ) by quenching them for various temperature. This basically gives the relationship between atomic disorder and magnetism. As a result it is shown that atomic disorder at Co type disorder leads to degradation of magnetism in heusler phase. In B<sub>2</sub>-phase  $\text{Co}_{1-x}\text{Fex}$  and  $\text{CoFe}_{1-x}\text{Al}_x$  alloys it was that proceeding of atomic disorder on Co site, Co-type disorder leads to a certain decrease in their mean magnetic moment. On the other hand, heusler phase  $\text{CoFe}_{1-x}\text{Al}_x$  alloys around the stoichiometry composition  $\text{Co}_2\text{FeAl}$  ( $x=0.5$ ) it was that the mean magnetic remains almost constant irrespective of atomic disorder between the Fe atomic disorder between the Fe and Al sites. Therefore this type of disorder affects hardly the magnetism. It is an interesting subject to clarify such a role of atomic disorder on the magnetism in various alloys  $\text{Co}_2\text{MnGe}$ . In this work however one problem remains to be solved namely about the change in lattice constant ( $a$ ) with quenching temperature,  $T_Q$  in fig2 shows a result for these alloys. The lattice constant decrease with increase in temperature up to 1073k  $\text{Co}_2\text{MnSi}$  while  $\text{Co}_2\text{MnGe}$  rather slowly in the form of former and steeply in the latter, while in  $\text{Co}_2\text{MnSn}$  it shows a steep decrease up to 1273k. Further an anomalous change in ( $a$ ) occur in  $\text{Co}_2\text{MnSi}$ ,  $\text{Co}_2\text{MnSi}$ , and  $\text{Co}_2\text{MnGe}$ . Therefore the curve shows an inflection above 1073k.

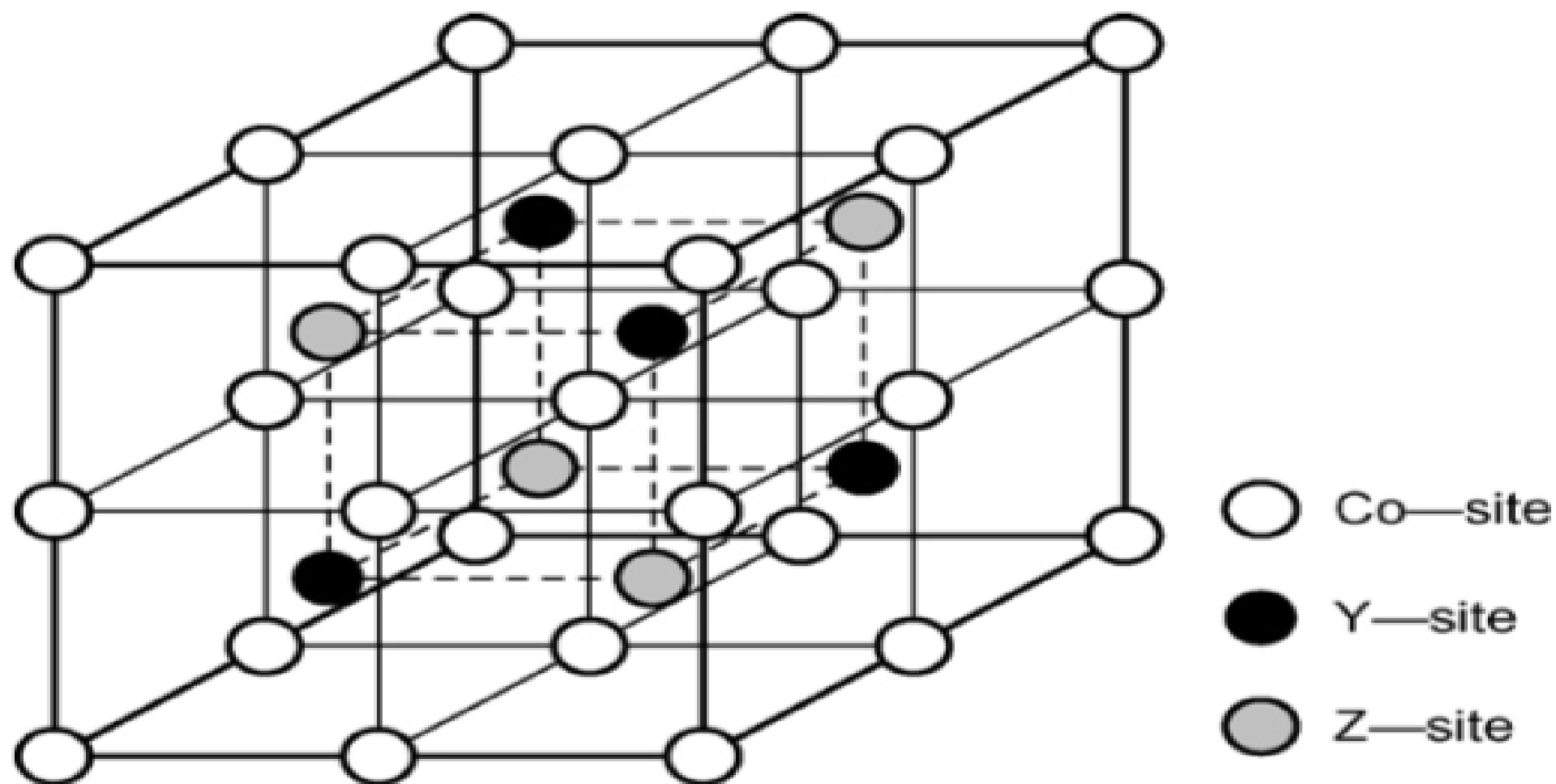


**Fig. 1.**  $\text{Co}_2\text{YZ}$  Heusler ( $\text{L2}_1$ )-type ordered structure.

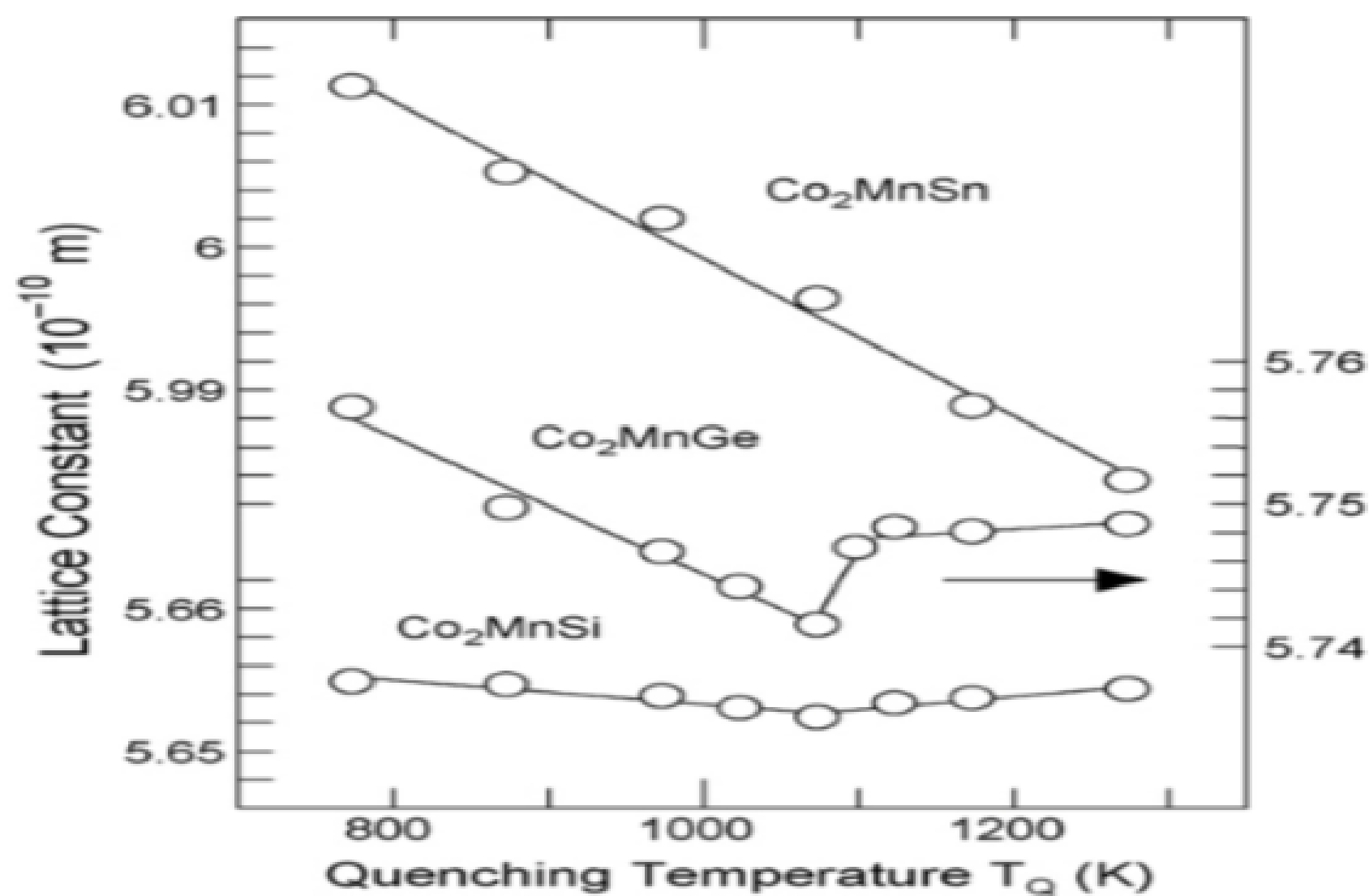


**Fig. 2.** Quenching temperature dependence of the lattice constant  $a$  in  $\text{Co}_2\text{MnSi}$ ,  $\text{Co}_2\text{MnGe}$  and  $\text{Co}_2\text{MnSn}$  alloys. These data are quoted from Ref. [10].

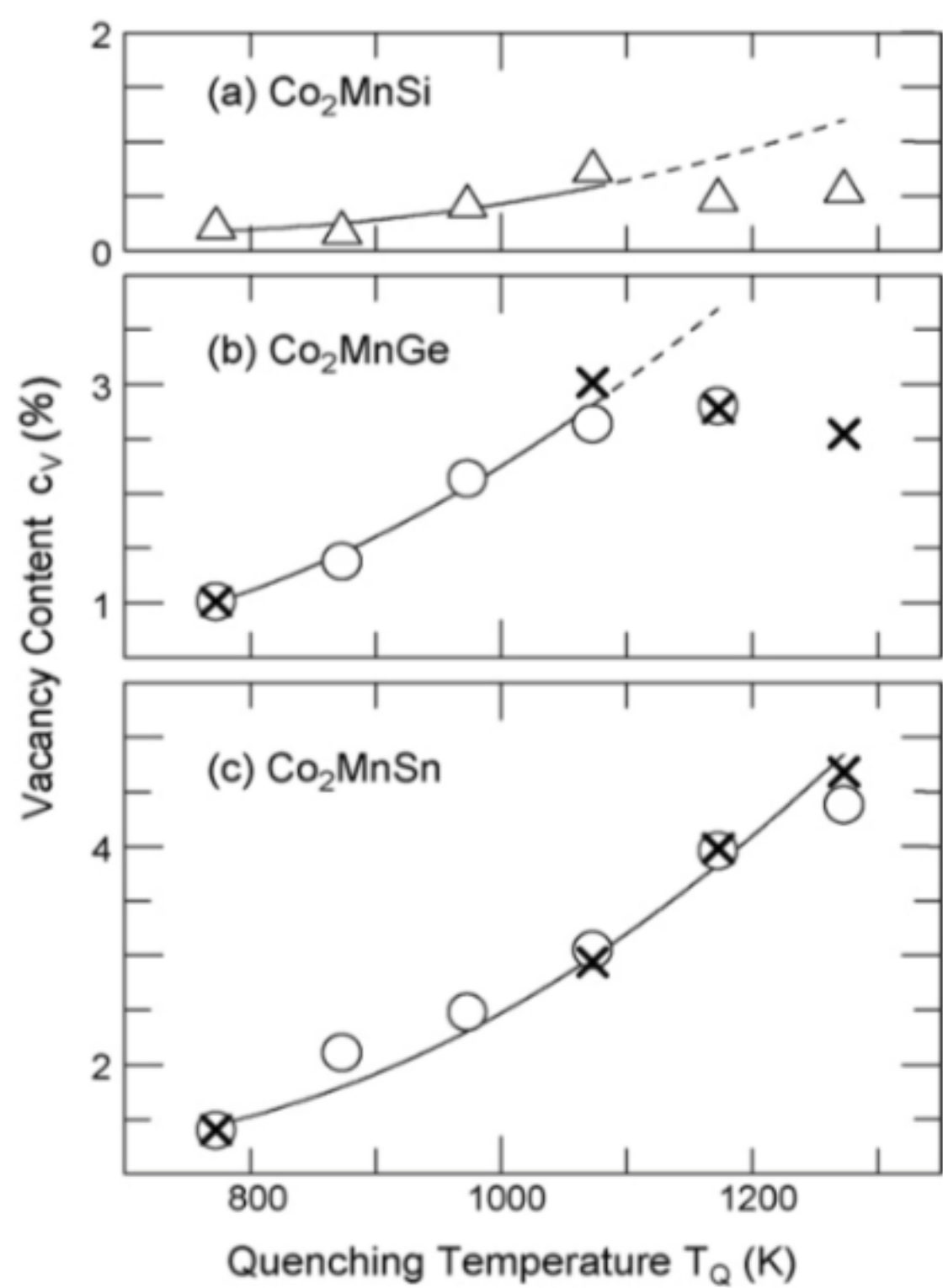
## 2. Experimental procedures

$\text{Co}_2\text{MnZ}$  ( $Z = \text{Si}, \text{Ge}$  and  $\text{Sn}$ ) alloys were prepared by arc melting Co and Mn (purity of 99.99%) and Si, Ge and Sn (99.999%). Weight losses were less than 0.5%. Each ingot was homogenized at 1273 K for 50 h in a sealed silica tube filled with argon. The plate samples with a size of about 10 mm  $\times$  5 mm  $\times$  1 mm were prepared for density measurement. They were annealed at 1173 K for 2 h in silica tubes filled with argon, followed by cooling to room temperature at a rate of 2 K/min. Individual samples were again annealed at

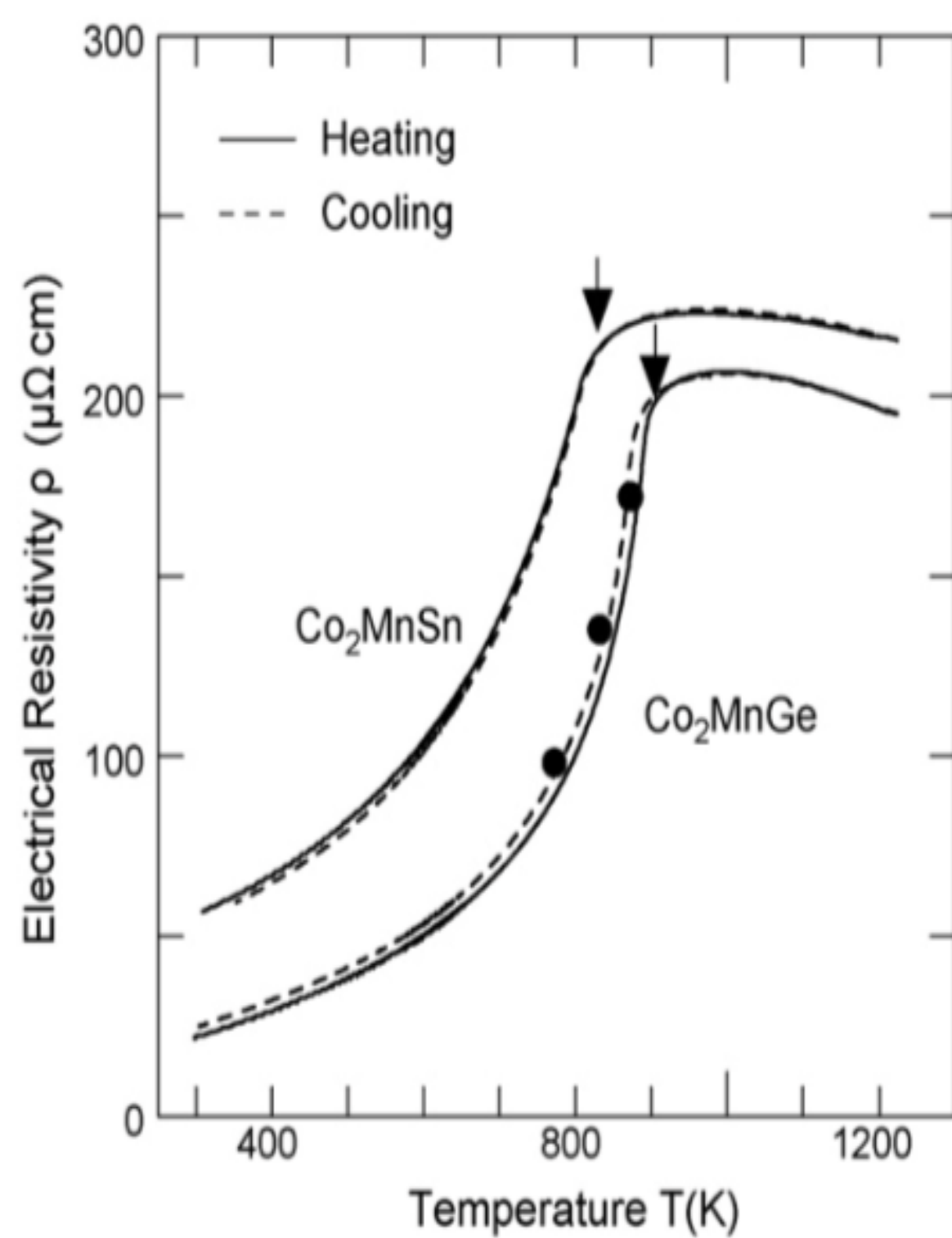
various temperatures from 773 K to 1273 K and then water-quenched (in quenching from temperatures above 973 K, the silica tubes were immediately crushed in water). Quenching temperature TQ and holding time are, 773 K (25–50 d), 873 K (14–21 d), 973 K (5–7 d), 1073 K (24 h), 1173 K (5 h) and 1273 K (1 h). The density measurement was performed based on the Archimedes method using distilled water in the same way as described. The vacancy concentration,  $C_v$ , can be obtained from

$$C_v = \frac{N_v}{N + N_v} = \frac{d_x - d_{\text{obs}}}{d_x}.$$

The deviations of  $C_v$  (%) were 1.2% in  $\text{Co}_2\text{MnGe}$  and 0.3% in  $\text{Co}_2\text{MnSn}$ . Consequently, for all the  $C_v$  data by the plate first water-quenched from 1173 K in a similar way as in the density measurement (without crushing silica tube) and then, after heated from room temperature to 773 K at a rate of



about



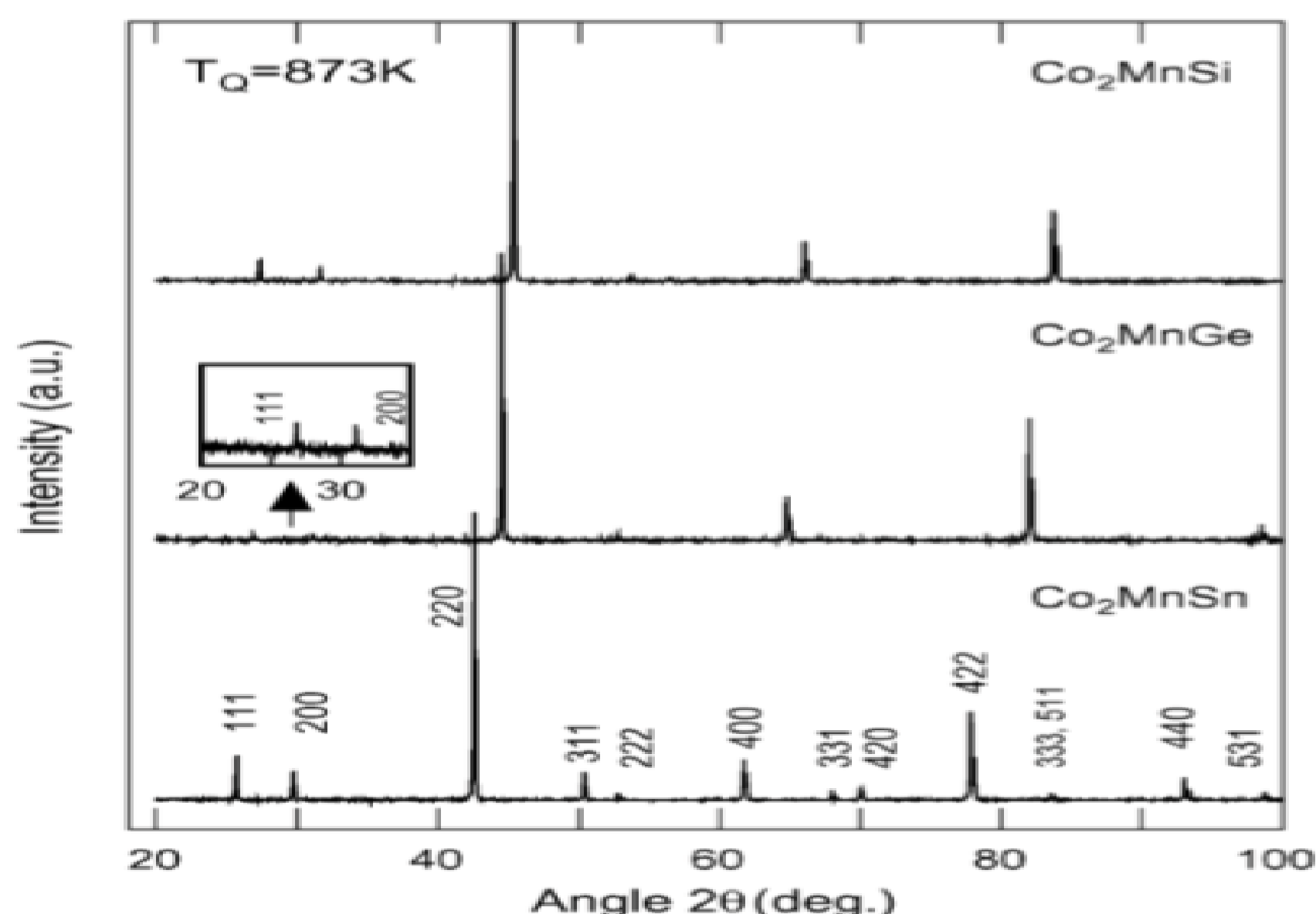
70K/min, the measurement was started.

Further, the other plate samples (about 5 mm × 5 mm × 1 mm) for positron annihilation measurements were prepared for Co<sub>2</sub>MnSi, Co<sub>2</sub>MnGe and Co<sub>2</sub>MnSn. As reference samples, plate samples of pure Co, Mn, Si, Ge and Sn were also prepared for the CDB measurement. The positron lifetime and CDB spectra consisted of  $1.0 \times 10^6$  and more than  $10^9$  counts, respectively.

## 2.2. Procedure for atomic disorder determination

### 2.2.1. Definition of the LRO-parameters and the Co-type and Y–Z-type defect concentrations

The point defect structure in the Co<sub>2</sub>YZ-type Heusler alloy can be described by specifying nine concentrations of constituent atoms on respective sites: three for the right atoms, e.g., Co atom on the Co-site, and six for the antisite atoms, e.g., Y atom on the Z-site and Z atom on the Y-site. Among these, number of the independent variables is four, so that four long-range order (LRO) parameters are generally needed for description of the defect structure. Here, for simplicity, we will follow the defect model adopted in our previous studies for CoFe<sub>1-x</sub>Al<sub>x</sub> Heusler alloys, which is based on the model proposed by Webster in neutron diffraction study. Then, the number of the LRO-parameters is reduced to two.

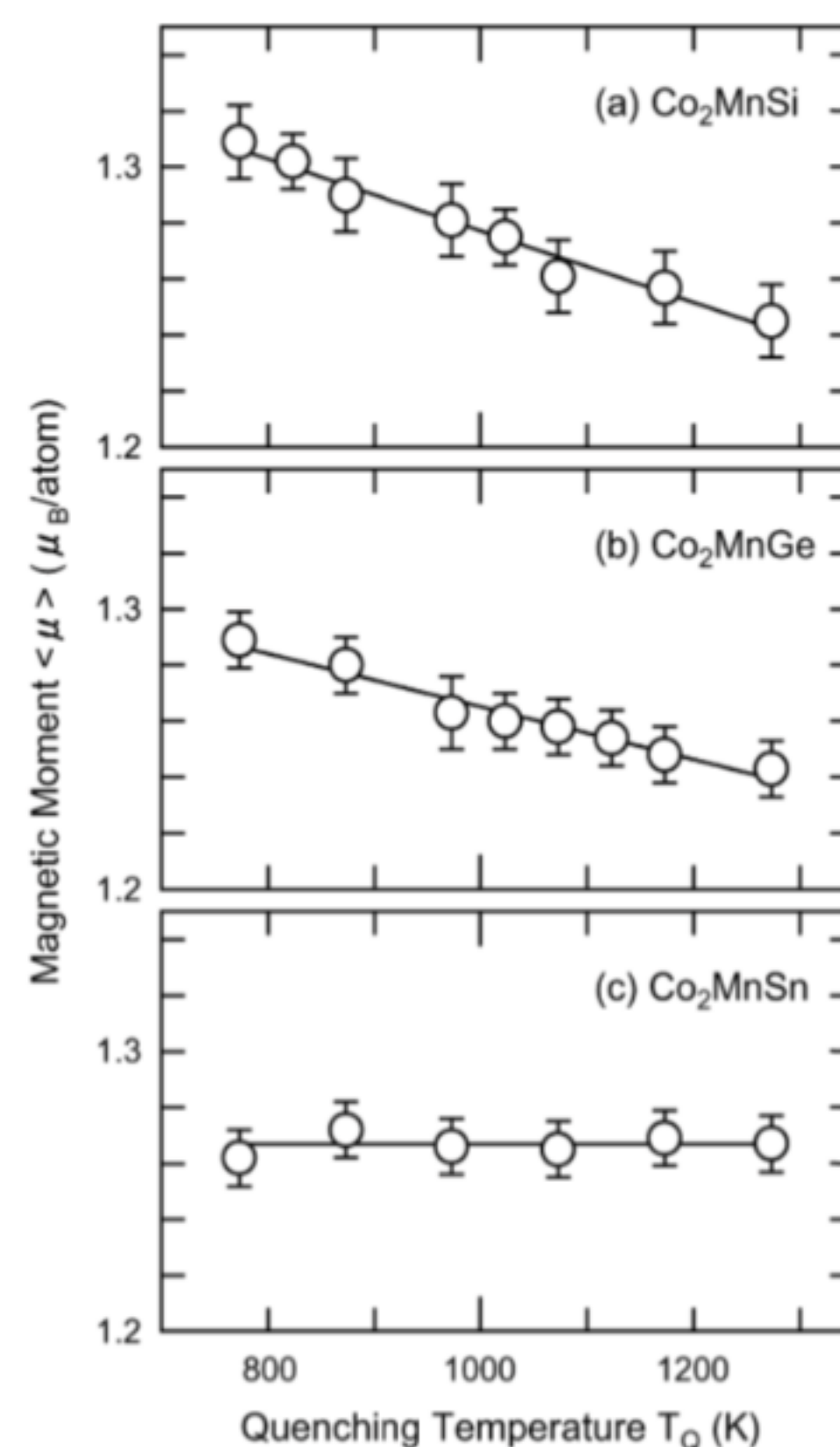
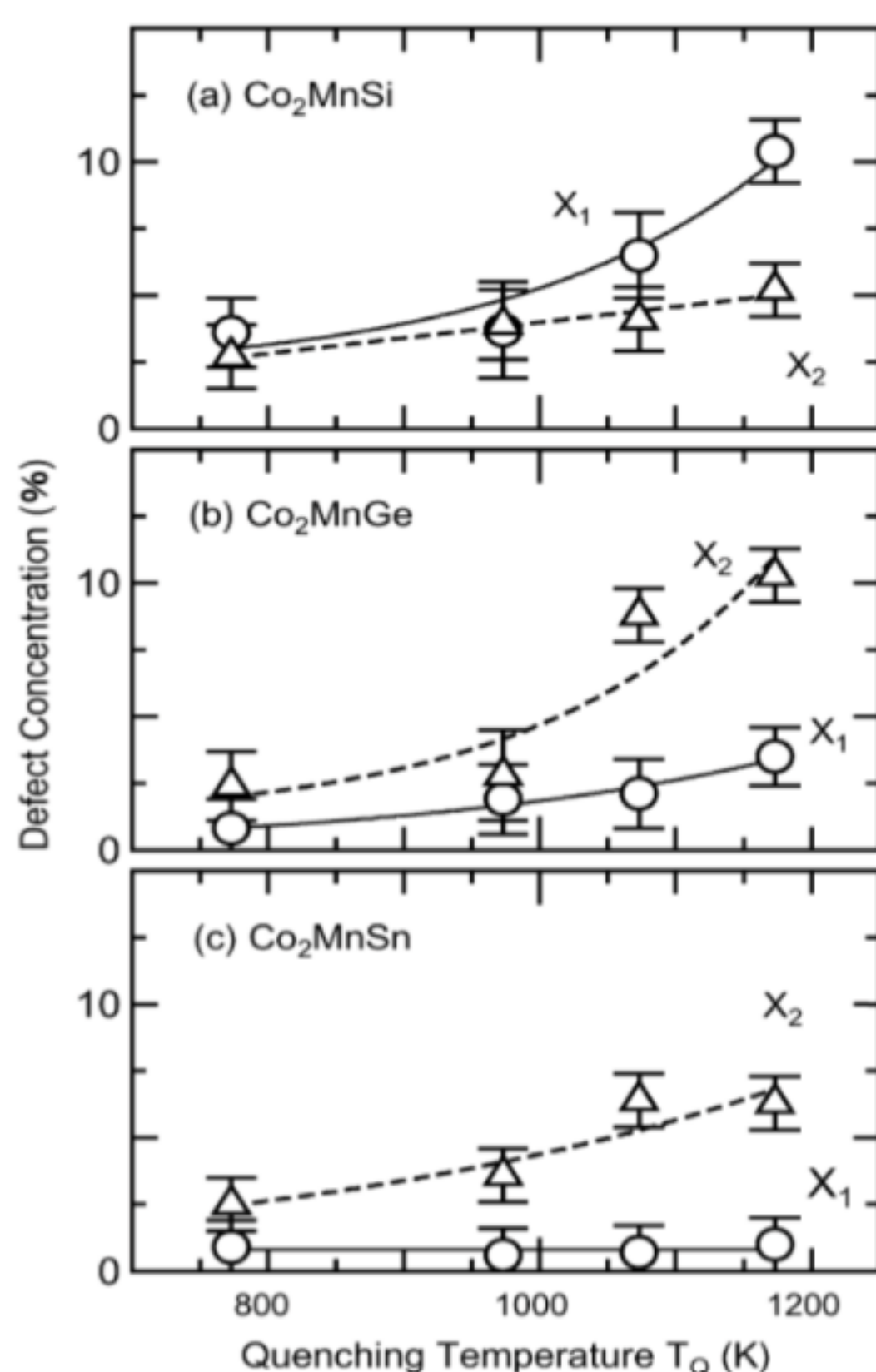




### 3. Results

#### 3.1. Lattice constant

The quenching temperature dependence of the lattice constant,  $a$ , is shown by the open circles in Fig. 4 for  $\text{Co}_2\text{MnSi}$  in Fig. 4(a),  $\text{Co}_2\text{MnGe}$  in Fig. 4(b) and  $\text{Co}_2\text{MnSn}$  in Fig. 4(c). The lattice constant shows a decrease with increase in quenching temperature  $T_Q$  up to 1073 K in both alloys  $\text{Co}_2\text{MnSi}$  and  $\text{Co}_2\text{MnGe}$ . The slope is however, very gradual for the former and steep for the latter. In  $\text{Co}_2\text{MnSn}$ , it decreases steeply (nearly the same slope as in the  $\text{Co}_2\text{MnGe}$ ) up to 1273 K. Two cross marks at  $T_Q = 773$  K and 1073 K in Fig. 4(a) represent the data by Ravel et al. [14]. Agreement with the present results is good. Further, the values of  $a$  reported by Webster are close to the present data at 973 K in Fig. 4(a)–(c). Another feature to be noted in  $\text{Co}_2\text{MnSi}$  (Fig. 4(a)) and  $\text{Co}_2\text{MnGe}$  (Fig. 4(b)) is that anomalous change in the lattice constant occurs, i.e., the curves show an inflection above 1073 K.



#### 3.2. Atomic disorder

Fig. 5 shows the quenching temperature dependence of the defect concentrations  $X_1$  (open circles) and  $X_2$  (open triangles) for  $\text{Co}_2\text{MnSi}$  in Fig. 5(a),  $\text{Co}_2\text{MnGe}$  in Fig. 5(b) and  $\text{Co}_2\text{MnSn}$  in Fig. 5(c). Both defect concentrations are found to increase with increase in quenching temperature in  $\text{Co}_2\text{MnSi}$  and  $\text{Co}_2\text{MnGe}$ . However, in  $\text{Co}_2\text{MnSi}$ , the slope is rather steep in  $X_1$  than in  $X_2$  and thus, the concentration  $X_1$  becomes much higher than  $X_2$  at higher quenching temperatures ( $T_Q > 973 \text{ K}$ ), while just reversed situation is recognized in  $\text{Co}_2\text{MnGe}$ . Namely, it can be said that the Co-type disorder preferentially proceeds in  $\text{Co}_2\text{MnSi}$  alloy as the quenching temperature increases, whereas in  $\text{Co}_2\text{MnGe}$  alloy, the Mn–Ge-type disorder preferentially proceeds. On the other hand, in  $\text{Co}_2\text{MnSn}$  alloy,  $X_1$  is very small and remains almost constant and so, only the Mn–Sn-type disorder occurs in practice. The same behavior was also observed in Heusler-phase  $\text{CoFe}_{1-x}\text{Al}_x$  alloys ( $0.4 \leq x \leq 0.6$ ). Webster and Brown et al. have studied the atomic disorder in present Heusler alloys by neutron diffraction measurement. According to their results,  $\text{Co}_2\text{MnSi}$  and  $\text{Co}_2\text{MnSn}$  alloys are highly ordered ( $X_1 = X_2 \approx 0\%$ ), but a small degree of disorder between the Mn- and Ge-sites ( $X_2 \approx 4\%$ ) is detected in  $\text{Co}_2\text{MnGe}$  alloy. These results correspond fairly well to the present observation at lower quenching temperatures ( $T_Q \leq 973 \text{ K}$ ), although the present  $X_1$  and  $X_2$  are somewhat larger in  $\text{Co}_2\text{MnSi}$  (Fig. 5(a)). Further, Rabel et al. obtained the defect concentrations for  $\text{Co}_2\text{MnSi}$  alloys quenched from 773 K and 1073 K by neutron diffraction measurement. The results were,  $X_1 = 6.9\%$  and  $X_2 = 0\%$  at  $T_Q = 773 \text{ K}$  and  $X_1 = 7.4\%$  and  $X_2 = 0\%$  at  $T_Q = 1073 \text{ K}$ . Their results of  $X_2 = 0\%$  come from the situation that all the Si-sites are exclusively occupied by Si atoms. Thus, the change in  $X_1$  mentioned above is due to proceeding of disorder between the Co- and Mn-sites (Co–Mn-type disorder). When only this type of disorder occurs, ordinary X-ray diffraction method, used in the present study, cannot give any information because of the small difference in atomic scattering factors between Co and Mn atoms. However, it can give rather correct information about the concentrations of the antisite Co and Mn atoms on the Si-site ( $x_{\text{Si Co}}$  and  $x_{\text{Si Mn}}$ ). Our results showed that e.g., the concentration  $x_{\text{Si Co}}$  increases certainly from 3.6% at  $T_Q = 773 \text{ K}$  to 10.4% at  $T_Q = 1173 \text{ K}$ ,



resulting in the changes in  $X_1$  and  $X_2$  shown in Fig. 5(a) (cf. Fig. 3(a)). The reason of this discrepancy is not clear, although it may come from the difference in some factors relating to the experimental method and the sample preparation.

### 3.3. Mean magnetic moment

The quenching temperature dependence of the mean magnetic moment is shown by the open circles in Fig. 6 for  $\text{Co}_2\text{MnSi}$  in (a),  $\text{Co}_2\text{MnGe}$  in Fig. 6(b) and  $\text{Co}_2\text{MnSn}$  in Fig. 6(c). The magnetic moment decreases with increase in quenching temperature in  $\text{Co}_2\text{MnSi}$  and  $\text{Co}_2\text{MnGe}$ , rather gradually for the latter compared with the former. On the other hand, in  $\text{Co}_2\text{MnSn}$ , remains almost constant. Webster has previously measured the magnetic moment for various  $\text{Co}_2\text{MnZ}$  alloys. Obtained values of are 1.27 for  $\text{Co}_2\text{MnSi}$  and  $\text{Co}_2\text{MnSn}$  and 1.28 for  $\text{Co}_2\text{MnGe}$  in atom unit, which are close to the present results at  $TQ = 1023$  K for  $\text{Co}_2\text{MnSi}$  and at  $TQ = 873$  K for  $\text{Co}_2\text{MnGe}$  and, agree well with that for  $\text{Co}_2\text{MnSn}$ .

### 3.4. Vacancy concentration

The quenching temperature dependence of the vacancy concentration  $C_v$  is shown in Fig. 3 for  $\text{Co}_2\text{MnSi}$  in (a),  $\text{Co}_2\text{MnGe}$  in (b) and  $\text{Co}_2\text{MnSn}$  in (c). The open triangles and cross-marks represent the results obtained for the plate samples and the powder samples, respectively. As mentioned in previous section, the plate sample data are corrected for  $\text{Co}_2\text{MnGe}$  and  $\text{Co}_2\text{MnSn}$ , which are plotted by the open circles (Fig. 3(b) and (c)). Agreement with corresponding powder sample data is good. The solid and dotted curves represent the fitting curves, which are mentioned in later Section 3.4.1. The vacancy concentration  $C_v$  increases with increase in quenching temperature  $TQ$  up to 1073 K in  $\text{Co}_2\text{MnSi}$  and  $\text{Co}_2\text{MnGe}$  and up to 1273 K in  $\text{Co}_2\text{MnSn}$ . The slope is rather gradual for  $\text{Co}_2\text{MnSi}$ , while very steep for  $\text{Co}_2\text{MnGe}$  and  $\text{Co}_2\text{MnSn}$ , corresponding well to the observed trend in the lattice constant  $a$  shown in Fig. 2. Furthermore, in  $\text{Co}_2\text{MnSi}$  (Fig. 3(a)) and  $\text{Co}_2\text{MnGe}$  (Fig. 3(b)), reduction of  $C_v$  values from the dotted curves is recognized above 1073 K, which just corresponds to the inflection found in  $a$  of these alloys (Fig. 2).

Therefore, it can be said that there is a certain correlation between changes in the vacancy concentration and the lattice constant in the present Heusler alloys.

### **3.5. Electrical resistivity**

Prior to the ageing experiment, we have measured the change in electrical resistivity, with temperature,  $T$ , for  $\text{Co}_2\text{MnGe}$  and  $\text{Co}_2\text{MnSn}$ , at heating and cooling rates of 2 K/min. The results are shown in Fig. 4 by the solid curves (heating process) and dotted ones (cooling process). In both alloys, an inflection is clearly found, which will be due to a magnetic transition since the inflection points are close to the Curie temperature,  $T_C$ , shown by the arrows. A feature to be noted is that the resistivity shows a slight decrease after reaching its maximum above  $T_C$ . Such a negative temperature dependence of  $\rho$  in a range  $T > T_C$  has been already reported in some D03-type ferromagnetic ternary alloys  $(\text{Fe}_{1-x}\text{M}_x)_3\text{X}$  (e.g.,  $\text{X} = \text{Ga}$  and  $\text{Si}$ , and  $\text{M} = \text{Ti}$  and  $\text{V}$ ).

## **4. Conclusion**

The Co-type and Mn–Z-type atomic disorder, the magnetic behavior and thermal vacancy were studied for three Heusler-type ferromagnetic alloys  $\text{Co}_2\text{MnZ}$  ( $\text{Z} = \text{Si}$ ,  $\text{Ge}$  and  $\text{Sn}$ ) as a function of quenching temperature. Concluding remarks are as follows:

(1) Both the Co-type and Mn–Z-type defect concentrations increased with increase in quenching temperature in  $\text{Co}_2\text{MnSi}$  and  $\text{Co}_2\text{MnGe}$ . However, the change in the former is rather steep than in the latter in  $\text{Co}_2\text{MnSi}$ , while the reversed situation is found in  $\text{Co}_2\text{MnGe}$ . Namely, the Co-type disorder preferentially proceeds in  $\text{Co}_2\text{MnSi}$ , while the Mn–Ge-type disorder preferentially proceeds in  $\text{Co}_2\text{MnGe}$ . In  $\text{Co}_2\text{MnSn}$ , only the Mn–Sn-type disorder proceeds in practice.

(2) The mean magnetic moment decreased with increase in quenching temperature for  $\text{Co}_2\text{MnSi}$  and  $\text{Co}_2\text{MnGe}$ , while it remained almost constant in  $\text{Co}_2\text{MnSn}$ .

(3) Relation between the atomic disorder and the magnetic behavior was examined. It is concluded that the Co-type disorder leads to degradation of the magnetism as observed in  $\text{Co}_2\text{MnSi}$  and  $\text{Co}_2\text{MnGe}$ , while the Mn–Z-type disorder affects hardly the magnetism as in  $\text{Co}_2\text{MnSn}$ .

(4) The vacancy concentration determined from the density and lattice constant measurements increased with increase in quenching temperature up to 1073 K or 1273 K.

(5) Change in the electrical resistivity due to ageing at various temperatures of 773–873 K showed a relaxation behavior in  $\text{Co}_2\text{MnGe}$  and  $\text{Co}_2\text{MnSn}$ . This is due to annealing-out of the excess vacancies retained during furnace-cooling from 1173 K.

## References

- [1] Y. Miura, K. Nagao, M. Shirai, Phys. Rev. B69 (2004) 144413.
- [2] S. Picozzi, A. Continenza, A.J. Freeman, Phys. Rev. B69 (2004) 094423.
- [3] Y. Miura, M. Shirai, K. Nagao, J. Appl. Phys. 99 (2006) 08J112.
- [4] I. Galanakis, K. Ozdogan, B. Aktas, E. Sasioglu, Appl. Phys. Lett. 89 (2006) 042502.
- [5] K. Harada, H. Ishibashi, M. Kogachi, Mater. Res. Soc. Symp. Proc. 753 (2003), BB5.28.1.
- [6] M. Kogachi, S. Minamigawa, K. Nakahigashi, Acta Metall. Mater. 40 (1992) 1113.
- [7] M. Kogachi, T. Tanahashi, Scripta Mater. 35 (1996) 849.
- [8] R. Wurschum, C. Grupp, H.E. Schaefer, Phys. Rev. Lett. 75 (1995) 97.
- [9] H.E. Schaefer, K. Bedula-Gergen, Defect Diff. Forum 143–147 (1997) 193.

[10] M.S. Wechsler, Acta Metall. 5 (1957) 150.

[11] A. Broska, J. Wolff, M. Franz, Th. Hehenkamp, Intermetallics 7 (1999) 259.

[12] M. Kogachi, High Temp. Mater. Process. 18 (1999) 269.

[13] H.E. Schaefer, Proceedings of the International Conference on Positron Annihilation, 1985, p. 448